Ampère force exerted by geomagnetic Sq currents and thermospheric pressure difference

AUTHOR(S):

Takeda, Masahiko

CITATION:

Takeda, Masahiko. Ampère force exerted by geomagnetic Sq currents and thermospheric pressure difference. Journal of Geophysical Research: Space Physics 2015, 120(5): 3847-3853

ISSUE DATE:

2015-05-06

URL:

http://hdl.handle.net/2433/201538

AGU PUBLICATIONS
JGR
Journal of Geophysical Research: Space Physics

RESEARCH ARTICLE
10.1002/2014JA020952

Key Points:
- The Ampère force by *Sq* currents highly correlates with the pressure difference
- These two values around the *Sq* current center are almost the same in equinox
- The pressure difference is smaller than the Ampère force in summer

Correspondence to:
M. Takeda,
takeda@kugi.kyoto-u.ac.jp

Citation:
Takeda, M. (2015), Ampère force exerted by geomagnetic *Sq* currents and thermospheric pressure difference, *J. Geophys. Res. Space Physics*, *120*, 3847–3853, doi:10.1002/2014JA020952.

Received 18 DEC 2014
Accepted 1 APR 2015
Accepted article online 8 APR 2015
Published online 6 MAY 2015

Ampère force exerted by geomagnetic *Sq* currents and thermospheric pressure difference

Masahiko Takeda[1]

[1]Data Analysis Center for Geomagnetism and Space Magnetism, Faculty of Science, Kyoto University, Kyoto, Japan

Abstract The Ampère force exerted by meridional *Sq* currents was estimated, and its relationship with a neutral pressure difference was examined. It was found that the annual Ampère force correlates very well with the difference between its maximum and minimum pressures integrated above 120 km for solar activity variation. Furthermore, these two values were almost the same around the *Sq* current vortex during the equinox. This means that the pressure difference balances with Ampère force, and thus, a neutral wind blows roughly in the opposite direction of the pressure gradient. As a result, the intensity of the resultant ionospheric dynamo current is controlled by the pressure difference, and thus, it is possible to infer the pressure difference from the geomagnetic field only at least the annual mean in equinox. At Kakioka, there was seasonal variation such that the pressure difference in the local summer and winter was smaller and larger than the Ampère force, respectively. This characteristic is likely due to the contribution of the interhemispheric field-aligned currents driven by the ionospheric dynamo to the *Sq* field.

1. Introduction

Solar quiet daily geomagnetic field variation (*Sq*) is primarily caused by ionospheric dynamo currents (j). These dynamo currents are first driven by the dynamo electric field ($V \times B$) generated by the interaction of neutral wind (V) with the geomagnetic main field (B) and create the electrostatic field by charging from the initial dynamo currents. As a result, the electric current is also driven by the electrostatic field that was developed to avoid excess changing. On the other hand, the electric current exerts an Ampère force (AF) ($j \times B$) on the atmosphere, and thus, the ionospheric dynamo is important not only in the geomagnetic *Sq* field but also in the dynamics of the neutral atmosphere.

Fukushima [1979] presented a schematic mechanism for the generation of *Sq* currents, in which neutral winds blow in the direction opposite the pressure gradient. However, in order to generate such winds, it is necessary for the pressure gradient force to be balanced not with a Coriolis force but with a drag force. In other words, the drag force should overcome the Coriolis force. If this condition is satisfied, the strength of the *Sq* currents can be used as an indicator of the pressure gradient of the neutral atmosphere, including solar activity effects.

Long-term variation of the *Sq* field has long been studied by many researchers. Since *Chapman and Bartels* [1940], it has been widely accepted that the amplitude of the *Sq* field is strongly controlled by solar activity. In addition to this solar activity dependence, many researchers have examined the relations between the long-term variations in the *Sq* field and several other parameters such as the geomagnetic main field, geomagnetic activity, and neutral wind. For example, *Glassmeier et al.* [2004] examined the effects of long-term geomagnetic variation on the magnetospheric and ionospheric physics and emphasized the importance of the geomagnetic main field in studying the physics. *Clilverd et al.* [2005] reported that the long trend of the *Sq* field can be partly due to solar activity. The solar activity dependence of *Sq* variations is mainly due to the enhanced ionospheric conductivity during high solar activity periods, which lead to increased ionospheric currents [e.g., *Takeda et al.*, 2003]. *Le Mouël et al.* [2005] and *Macmillan and Droujinina* [2007] showed that the magnitude of *Sq* variations is mainly controlled by solar radiation activity even after the removal of solar cycle effects. *Yamazaki and Kosch* [2014] examined the long-term variation of *Sq* and lunar variation (L) and showed that both have basically the same dependence on solar activity, suggesting that both are strongly controlled by the ionospheric conductivity.

In the present study, the total intensities of the meridional *Sq* currents flowing above six observatories are first estimated from the time integration of the Y component of the *Sq* amplitude. Next, the AF exerted by

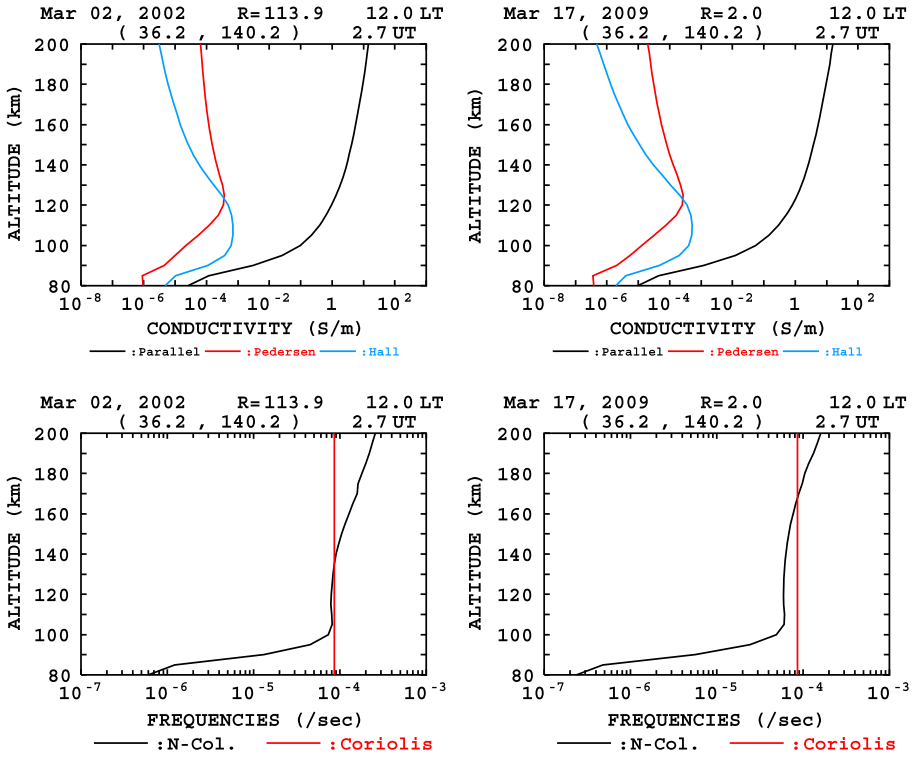

Figure 1. (top) The examples of height profiles of electric conductivity and (bottom) the neutral-ion collision frequency and the Coriolis parameter above Kakioka at noon. (left and right) The profiles for the solar maximum and minimum days, respectively.

the currents is calculated combining with the geomagnetic main field model and compared with the height-integrated neutral pressure difference (PD). Finally, the long-term variations of the AF and the PD and the relationship between them are discussed.

2. Data Analysis

In the present analysis, the total meridional *Sq* current (TJ) was first estimated from geomagnetic hourly values of the *Y* component and used to calculate the AF. The TJ was estimated from the hourly

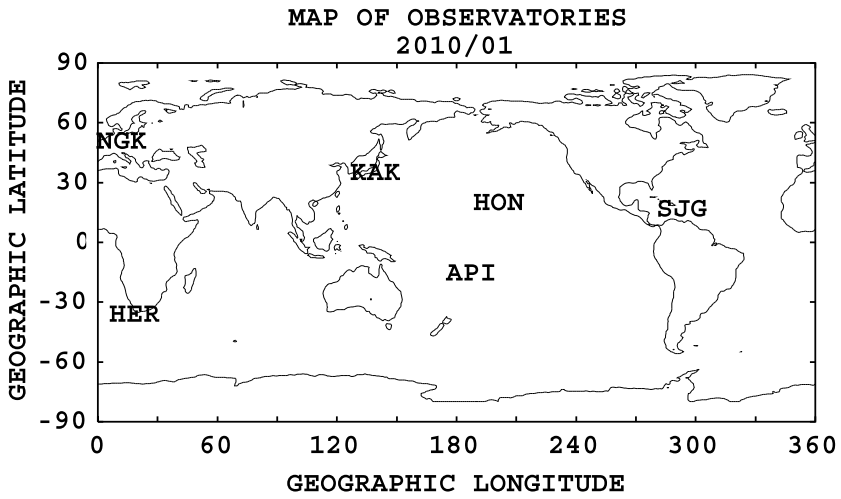

Figure 2. Geomagnetic observatories used in the present study.

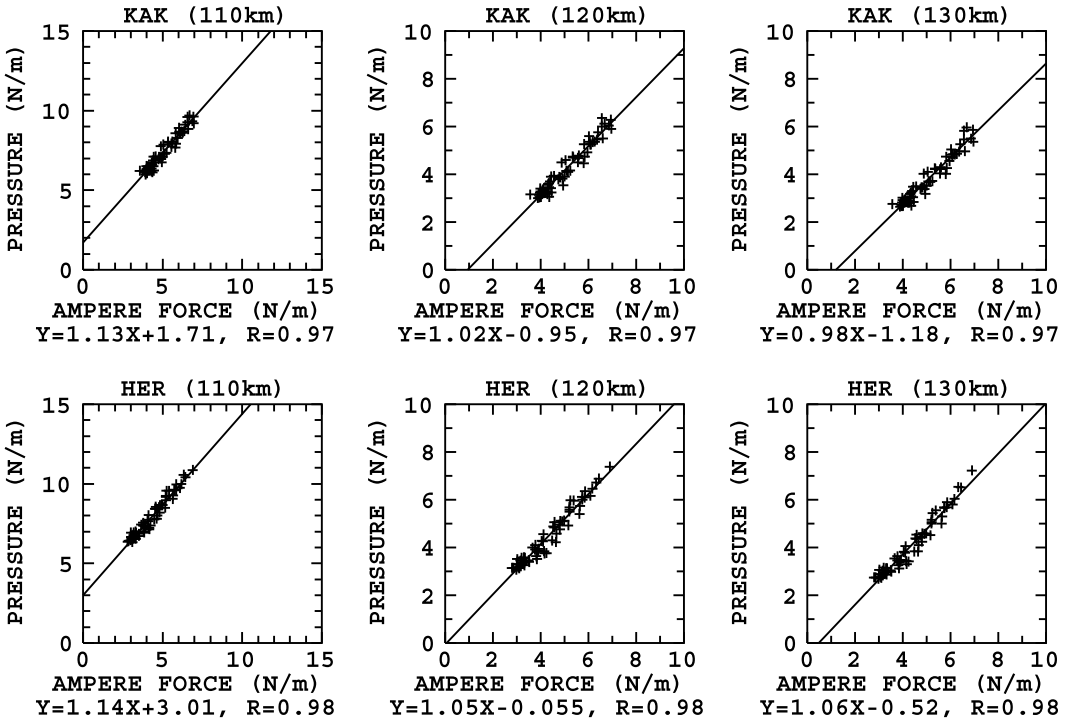

Figure 3. The correlation between the Ampère force and the pressure difference at (top) KAK and (bottom) HER during the equinoxes from 1947 to 2010. The cases in which the lower boundaries of the height integration are (left) 110, (middle) 120, and (right) 130 km, respectively. A linear regression line is drawn in each panel, and the linear regression equation and correlation coefficient are given at the bottom of each panel.

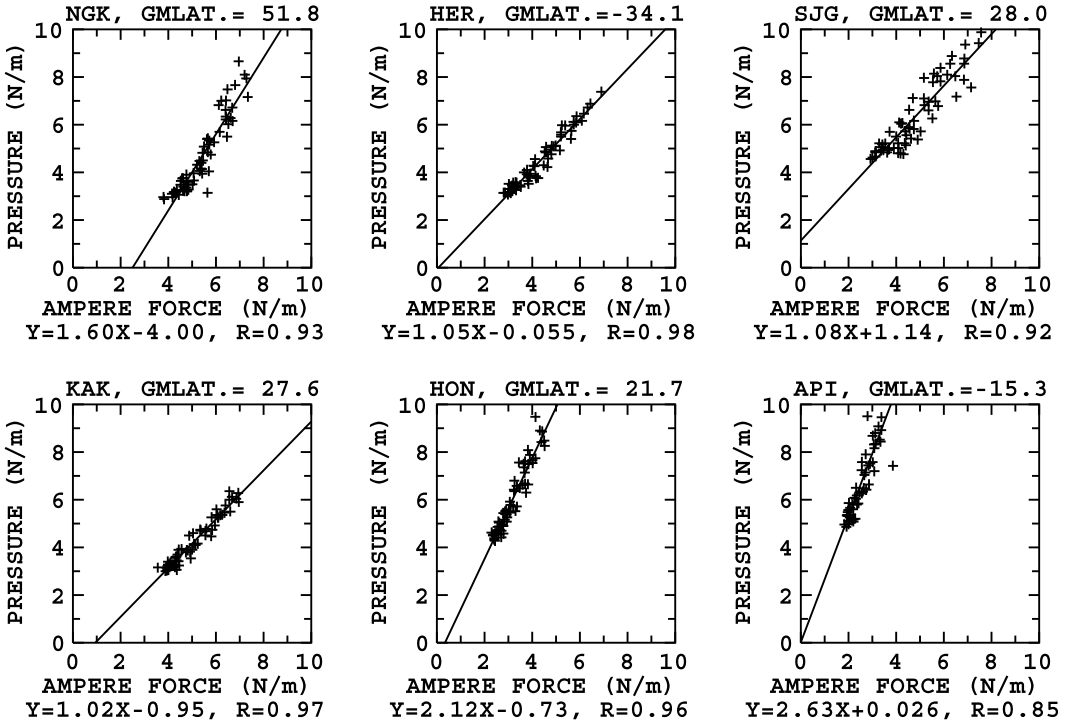

Figure 4. The correlation between the Ampère force and the pressure difference at NGK, HER, SJG, KAK, HON, and API during the equinoxes from 1947 to 2010. A linear regression line is drawn in each panel, and the linear regression equation and correlation coefficient are given at the bottom of each panel.

Y-component values of the geomagnetic field between 06:00 and 18:00 LT by summing their difference [*Y* (hour)] from the night value, which is the average between 21:00 and 02:00 LT on the same day, as

$$\mathrm{TJ} = \frac{4(R_E + h)\sum |Y(\mathrm{hour})| \cos\,\Theta}{2 \times 24 \times 3\ \ \mu_0}$$

where R_E is the Earth's radius (6370 km), h is the ionospheric height (assumed to be 120 km), Θ is the geomagnetic latitude, and μ_0 is the vacuum permeability ($4\pi \times 10^{-7}$ N/A^2). Here the coefficient 2 in the denominator is to get one-way meridional currents, and $(R_E + h)\cos\Theta/24$ corresponds to the horizontal length of 1 h in the ionosphere above the observatory. The factor of 3/4 is the conversion of the magnetic field variation in A/m to a height-integrated current density, assuming that the contribution of the induced current in the Earth to the geomagnetic *Sq* field is half that of the external current based on the results of the spherical harmonics analysis [*Takeda*, 2002]. The AF was estimated using the TJ and the geomagnetic field *Z* component (B_z) as

$$\mathrm{AF} = \mathrm{TJ} \times B_z$$

The PD was estimated as the difference between the maximum and minimum values of the height-integrated neutral pressure. First, the height distribution of the neutral atmospheric pressure for each hour on each day was calculated using the NRLMSISE-00 atmosphere model. Next, it was necessary to determine an adequate height range for the pressure integration, considering that the AF is exerted by height-integrated ionospheric currents. The importance of the AF in thermospheric dynamics could be estimated from the neutral-ion collision frequency and Coriolis parameters $2\Omega\sin\theta$, where Ω is the angular frequency of the Earth's rotation and θ is the geographic latitude, because the AF acts on the neutral atmosphere through the collisions of charged particles, especially ions. Figure 1 gives an example of a height profile of electric conductivity, where the neutral-ion collision frequency and Coriolis parameters above Kakioka were estimated by International Reference Ionosphere (IRI) 2012 [*Bilitza et al.*, 2011] and NRLMSISE-00 atmosphere models at noon on days when the solar activity was high and low, respectively. This figure shows that the collision frequency is smaller than the Colioris parameter below 110 km, the two are approximately equal in the height range between 110 and 160 km, and the collision frequency is larger for heights above 160 km. On the other hand, electric currents flow mainly below 130 km. Considering this situation, lower boundaries for the pressure integration between 110 and 130 km were tested. The higher boundary was set at 400 km, which is not so critical because pressure is very low at higher altitudes.

The geomagnetic observatories used in this analysis were Hermanus (HER), San Juan (SJG), Honolulu (HON), Kakioka (KAK), Niemegk (NGK), and Apia (API), and their locations are shown in Figure 2. These observatories were selected because their long-term data are relatively continuous and of good quality. The days used in the present analysis were those when *Kp* index did not exceed 3+ to avoid contamination of the geomagnetic disturbance field. The obtained AF and PD during the equinox (March, April, September, and October) and summer (May–August) and winter (December–February) solstices were averaged for each year and used in the subsequent analysis.

3. Results and Discussion

Figure 3 shows the correlation between the AF and PD at KAK and HER during the equinoxes from 1947 to 2010. The lower boundaries of the height integration were 110, 120, and 130 km. The correlation coefficients in all cases were found to be very high (≥0.97). In addition to these lower boundaries, the correlations between the PD and AF were checked using various lower boundary conditions. It was determined that 120 km was the best, and thus, the PD was integrated from 120 km in the analysis.

Figures 4 shows the correlations between the AF and PD at NGK, HER, SJG, KAK, HON, and API during the equinoxes from 1947 to 2010. A linear regression line is drawn in each panel, and the linear regression equation and correlation coefficient are given at the bottom of each panel. The correlation coefficients between the AF and PD are very high (≥0.85). However, the most important point is that the AF and PD values are almost equal at KAK, HER, and SJG. It is very surprising that two such independently obtained values were almost the same throughout the measurement period. This result supports the hypothesis included in the *Sq* generation mechanism proposed by *Fukushima* [1979]. That is, the fact that the AF is equal to the PD means that the PD is balanced not by the Colioris force but by the AF, and thus, winds blow in the opposite direction of the pressure gradient. As a result, the winds diverge from the subsolar point, as Fukushima proposed.

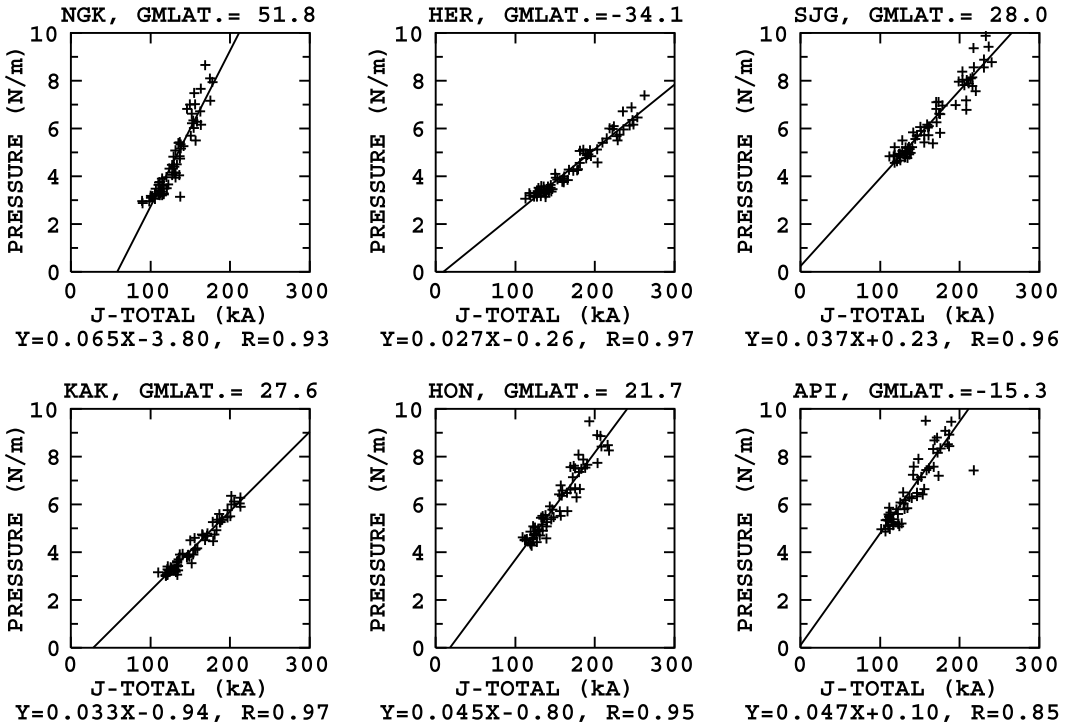

Figure 5. Same as Figure 4 but the correlation is between the total current and the pressure difference.

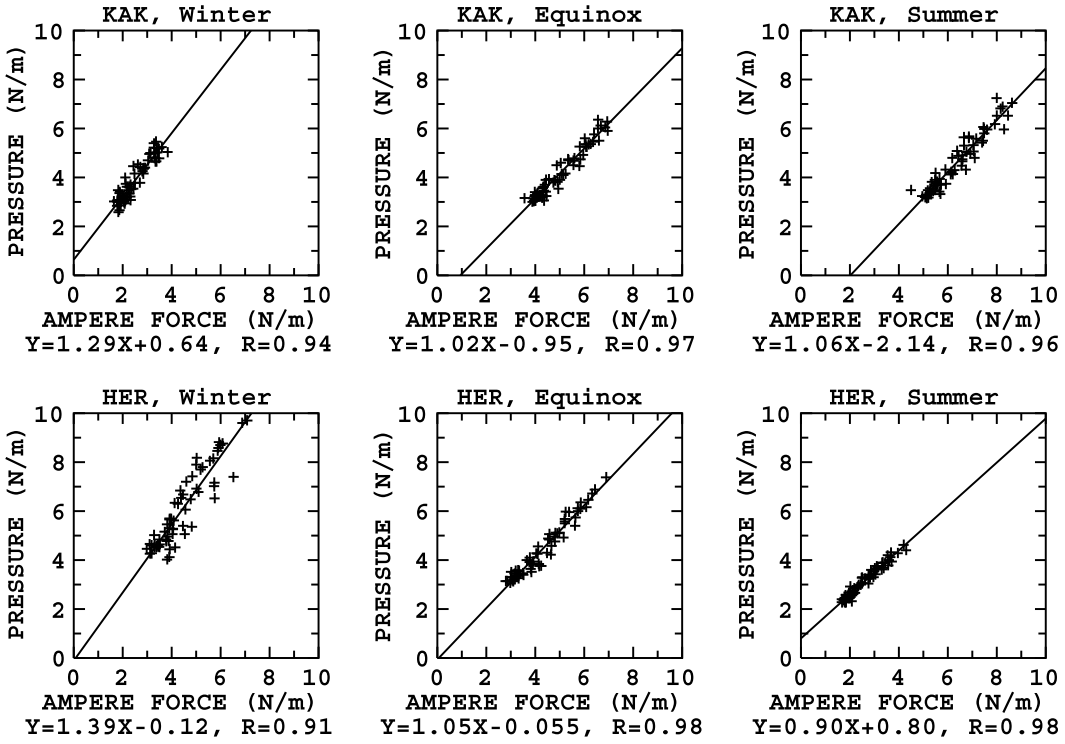

Figure 6. Seasonal variation of the correlation between the Ampère force and the pressure difference at (top) KAK and (bottom) HER during the (left) winter, (middle) equinox, and (right) summer. Note that winter and summer in this figure correspond to the local summer and winter, respectively, for HER in the southern hemisphere. A linear regression line is drawn in each panel, and the linear regression equation and correlation coefficient are given at the bottom of each panel.

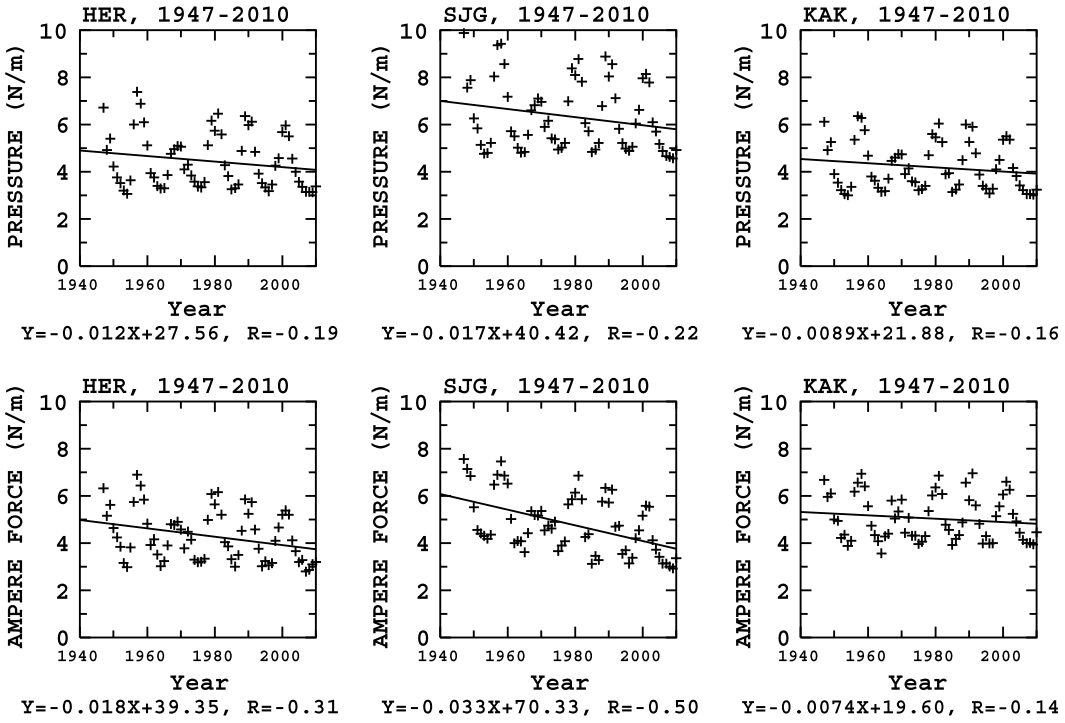

Figure 7. The (top) pressure difference and (bottom) Ampère force at (left) HER, (middle) SJG, and (right) KAK during the equinoxes from 1947 to 2010.

The fact that the PD and AF shows similar responses to solar activity variation means that the PD acts as a current generator for the *Sq* dynamo. When the PD increases due to the enhanced solar activity, the wind initially accelerates, but the ion drag force, which is the same as the AF in the dynamo region, subsequently increases and decelerates the wind to balance the AF and PD. In fact, *Takeda* [2013] showed that wind velocity decreases with higher solar activity, which may be interpreted as proof of the necessity of this balance, if ionospheric conductivity depends on solar activity more than the PD. Of course, the above discussion does not necessarily imply that the *Sq* dynamo acts as a current generator for the solar activity itself, because the linearity of the relation between the PD and solar activity is not guaranteed. On the other hand, a strong correlation suggests that the AF, which can be estimated by using geomagnetic data only, can be used as a proxy for PD. Moreover, the AF may be a better indicator of the thermosphere than sunspot number (SSN) or $F_{10.7}$ because the AF reflects the PD in the sense of "output" of the *Sq* dynamo and thus reflects the condition of the thermosphere, while SSN and $F_{10.7}$ represent the "inputs" of the thermosphere.

Although the correlation itself is still strong, the above-mentioned balance may not be realized at observatories further from the *Sq* current vortex, because the AF is smaller than the PD. In higher latitudes, it is probable because the effect of the Coriolis force increases and becomes more effective. On the other hand, it seems that the PD will probably balance with the force of inertia because the Coriolis force is not effective in lower latitudes. In fact, *Huang et al.* [2013] showed by numerical simulation that the phase of the zonal wind is delayed in lower latitudes, which suggests the greater importance of the inertial force there.

Figure 5 shows the correlations between the TJ and PD at NGK, HER, SJG, KAK, HON, and API during the equinoxes from 1947 to 2010. The correlations are approximately the same as those between the AF and PD. This result shows that the correlation between the AF and PD is almost due to that of the TJ and PD. However, the AF is likely a good indicator of the thermosphere because it is directly exerted on the neutral atmosphere, and thus, the AF was mainly used in the present study.

Figure 6 represents the seasonal variation of the correlation between the AF and PD at KAK and HER. Note that winter and summer here are defined as those in the northern hemisphere and correspond to the local summer and winter, respectively, for HER, which is in the southern hemisphere. This figure shows that the PD tends to be smaller than the AF in the local summer and vice versa in winter at KAK, although this trend is not so clear at HER.

This tendency at KAK can be explained by the effects of the magnetic field by interhemispheric field-aligned currents on the geomagnetic *Sq* field. That is, the *Sq* dynamo generates field-aligned currents directed from the hemisphere experiencing summer to the hemisphere experiencing winter in the morning and reversed currents in the afternoon [*Takeda*, 1982; *Yamashita and Iyemori*, 2002]. These field-aligned currents enhance the *Y* component of the *Sq* amplitude in the summer hemisphere and lower it in the winter hemisphere. On the other hand, the field-aligned current flows parallel to the magnetic field and does not contribute to the AF, and therefore, compared with the AF, the PD is larger in winter and smaller in summer.

Figure 7 shows the PD and AF at HER, SJG, and KAK during the equinoxes from 1947 to 2010. It can be found that the PD and AF fluctuate very similarly, showing clear 11 year solar cycle variations, which indicate a strong solar activity dependence. The linear trends show slight decreases in both the PD and AF at all observatories. However, since the solar activity tends to decrease during this period, this decrease likely reflects solar activity variation in this period [*Takeda*, 2013]. On the other hand, the rates of change of the PD and AF are both the largest at SJG and smallest at KAK. This similarity between the secular variations of the PD and AF at each site also supports the idea that the PD is a current generator for the *Sq* dynamo.

4. Conclusion

The relationship between the AF exerted by the ionospheric *Sq* current and the PD was examined by the TJ estimated from the *Y* component of the observed *Sq* field and the NRLMSISE-00 atmospheric model. The main results are summarized as follows:

1. The annual average AF obtained from the meridional *Sq* currents and the PD is very strongly correlated with variations in solar activity.
2. The AF and PD are approximately equivalent at observatories close to the *Sq* current vortex center during equinoxes.
3. This equality indicates that the explanation of the ionospheric *Sq* dynamo proposed by *Fukushima* [1979] is roughly appropriate and that the PD is a current generator for the ionospheric *Sq* dynamo.
4. During summer and winter, the PD at KAK is smaller and larger than the AF, respectively. This characteristic probably results from the *Y* component of the geomagnetic *Sq* field enhanced during the summer by the interhemispheric field-aligned currents driven by the ionospheric dynamo.

Acknowledgments
The author acknowledges the World Data Center for Geomagnetism, Kyoto (http://wdc.kugi.kyoto-u.ac.jp/index.html) and the observatories for obtaining the geomagnetic data (hourly values and *Kp* index) used in the present study. The data were originally supplied by Japan Meteorological Agency, U.S. Geological Survey, South African National Space Agency in South Africa, Adolf-Schmidt-Observatorium für Erdmagnetismus in Germany, and Institute of Geological and Nuclear Sciences Ltd. in New Zealand, which operate KAK, HON and SJG, HER, NGK, and API, respectively. IGRF model is available at http://www.ngdc.noaa.gov/IAGA/vmod/igrf.html. IRI2012 model and corresponding conductivity model are available at http://iri.gsfc.nasa.gov/ and http://wdc.kugi.kyoto-u.ac.jp/ionocond/sigcal/index.html, respectively. SSN and NRLMSISE-00 models are available at http://sidc.oma.be/ and http://ccmc.gsfc.nasa.gov/modelweb/atmos/nrlmsise00.html, respectively.

Alan Rodger thanks the reviewers for their assistance in evaluating this paper.

References

Bilitza, D., L.-A. McKinnell, B. Reinisch, and T. Fuller-Rowell (2011), The International Reference Ionosphere (IRI) today and in the future, *J. Geod.*, *85*, 909–920, doi:10.1007/s00190-010-0427-x.

Chapman, S., and J. Bartels (1940), *Geomagnetism*, vol. 2, Oxford Univ. Press, U. K.

Clilverd, M. A., E. Clarke, T. Ulich, J. Linthe, and H. Rishbeth (2005), Reconstructing the long-term aa index, *J. Geophys. Res.*, *110*, A07205, doi:10.1029/2004JA010762.

Fukushima, N. (1979), Electric potential difference between conjugate points in middle latitudes caused by asymmetric dynamo in the ionosphere, *J. Geomagn. Geoelectr.*, *31*, 401–409.

Glassmeier, K.-H., J. Vogt, A. Stadelmann, and S. Buchert (2004), Concerning long-term geomagnetic variations and space climatology, *Ann. Geophys.*, *22*, 3669–3677.

Huang, C. Y., P. A. Roddy, E. K. Sutton, R. Stonebackb, R. F. Pfaffc, L. C. Gentilea, and S. H. Delayd (2013), Ion-neutral coupling during deep solar minimum, *J. Atmos. Sol. Terr. Phys.*, *103*, 138–146, doi:10.1016/j.jastp.2012.11.009.

Le Mouël, J. L., V. Kossobokov, and V. Courtillot (2005), On long-term variations of simple geomagnetic indices and slow changes in magnetospheric currents: The emergence of anthropogenic global warming after 1990?, *Earth Planet. Sci. Lett.*, *232*, 273–286.

Macmillan, S., and A. Droujinina (2007), Long-term trends in geomagnetic daily variation, *Earth Planets Space*, *59*, 391–395.

Takeda, M. (1982), Three dimensional ionospheric currents and field aligned currents generated by the asymmetrical dynamo action in the ionosphere, *J. Atmos. Sol. Terr. Phys.*, *44*, 187–193.

Takeda, M. (2002), Features of global geomagnetic *Sq* field from 1980 to 1990, *J. Geophys. Res.*, *107*(A9), 1252, doi:10.1029/2001JA009210.

Takeda, M. (2013), Difference in seasonal and long-term variations in geomagnetic *Sq* fields between geomagnetic *Y* and *Z* components, *J. Geophys. Res. Space Physics*, *118*, 2522–2526, doi:10.1002/JGRA.50128.

Takeda, M., T. Iyemori, and A. Saito (2003), Relationship between electric field and currents in the ionosphere and the geomagnetic Sq field, *J. Geophys. Res.*, *108*(A5), 1183, doi:10.1029/2002JA009659.

Yamashita, S., and T. Iyemori (2002), Seasonal and local time dependences of the interhemispheric field-aligned currents deduced from the Ørsted satellite and the ground geomagnetic observations, *J. Geophys. Res.*, *107*(A11), 1372, doi:10.1029/2002JA009414.

Yamazaki, Y., and M. J. Kosch (2014), Geomagnetic lunar and solar daily variations during the last 100 years, *J. Geophys. Res. Space Physics*, *119*, 6732–6744, doi:10.1002/2014JA020203.